Enhancement of Interfacial Thermal Transport Between Metal and Organic Semiconductor Using Self-Assembled Monolayers With Different Terminal Groups

Journal:	*The Journal of Physical Chemistry*
Manuscript ID	jp-2020-02753u.R1
Manuscript Type:	Article
Date Submitted by the Author:	13-Jun-2020
Complete List of Authors:	Fan, Hongzhao; Shandong University, Institute of Thermal Science and Technology Wang, Man; Shandong University, Institute of Thermal Science and Technology Han, Dan; Shandong University, Institute of Thermal Science and Technology Zhang, Jingzhi; Shandong University, School of Energy and Power Engineering Zhang, Jingchao; Emory University, Wang, Xinyu; Shandong University, Institute of Thermal Science and Technology

Enhancement of interfacial thermal transport between metal and organic semiconductor using self-assembled monolayers with different terminal groups

Hongzhao Fan [1], Man Wang [1], Dan Han [1], Jingzhi Zhang [2], Jingchao Zhang [3], Xinyu Wang [1,*]

[1] Institute of Thermal Science and Technology, Shandong University, Jinan 250061, China

[2] School of Energy and Power Engineering, Shandong University, Jinan 250061, China

[3] Department of Biostatistics and Bioinformatics, Emory University, Atlanta, GA 30322, USA

Abstract

Inferior heat transfer between metal and organic semiconductor is a challenge for the performance improvement of organic semiconductor devices. In this paper, we use non-equilibrium molecular dynamics to study the thermal energy transport between the functionalized gold (Au) and pentacene interfaces. The functionalized modifications of Au surface are implemented by inserting four different self-assembled monolayers (SAMs) in the interface of Au and pentacene. Four different SAMs include 1-hexanethiol [$HS(CH_2)_5CH_3$], 6-aminohexane-1-thiol [$HS(CH_2)_6NH_2$], 6-mercapto-1-hexanol [$HS(CH_2)_6OH$] and 6-mercaptohexanoic acid [$HS(CH_2)_5COOH$]. The interfacial thermal conductance of bare Au interface is 8.91±2.45 MW m^{-2} K^{-1}. It is found that the interfacial thermal conductance can be enhanced by all four SAMs. The SAMs [$HS(CH_2)_5CH_3$ and $HS(CH_2)_6NH_2$] with a similar enhancement ability can improve the interfacial thermal conductance about 6~7 times. Moreover, the SAMs with stronger polarization groups [$HS(CH_2)_6OH$ and $HS(CH_2)_5COOH$] display the larger enhancement ability. Especially, the interfacial thermal conductance of the SAM

* Corresponding author, Email: xyw@sdu.edu.cn.

[$HS(CH_2)_5COOH$] functionalized Au interface is increased about 11 times. The enhancement of interfacial thermal transport is attributed to the better phonon vibrational coupling and the stronger interfacial interactions. SAMs can play the role of "phonon bridge" to connect the phonon density of states of Au and pentacene, which leads to the increase of interfacial thermal conductance at interface. The stronger polarization groups of SAMs bring about the higher adhesion energy and pull interfacial atoms closer to interface, which leads to smaller temperature drops and higher interfacial thermal conductance. The existences of hydrogen bonds are also observed for SAMs [$HS(CH_2)_6OH$ and $HS(CH_2)_5COOH$] functionalized interfaces, which are beneficial to the energy transfer at the interface. This work can provide a significant insight to tune thermal transport properties for organic electronic devices.

1. Introduction

Organic semiconductors, which are promising materials as the active layers, have been widely used to fabricate organic photovoltaics (OPVs), organic light-emitting diodes (OLEDs), biological sensing devices and organic field-effect transistors (OFETs)[1-3]. In comparison with using conventional inorganic semiconductors, OFETs using organic semiconductors can be conveniently manufactured at low temperature, low cost and high throughput[4-5]. Although organic semiconductors have many excellent properties, such as mechanical flexibility, versatile chemical design and synthesis, lightweight, biocompatibility and etc., the inferior charge transport performance caused by the nature of the weak van der Waals (vdW) interaction requests available techniques to improve the performance of organic semiconductors. Interface engineering is one of important techniques to improve the performance of organic electronic devices. In past two decades, many techniques such as chemical modifying[6], smoothing surface via polymer thin layers[7], utilizing hole-transporting buffer layers[8], inserting transition metal oxide[9] and functionalizing surface with self-assembled monolayers (SAMs)[10-15], have been vastly developed and implemented to manufacture high performance electronic devices. Because of the processability, high degree of order and versatility

of SAMs, molecular self-assembly has become an ideal way to reconcile inorganic and organic surfaces. Many physical properties, such as molecular orientation at interface[10, 11], carrier injection barrier[12-13, 16] and the quality of organic semiconductor films[11, 14-15, 17] can be optimized by modifying the interface with SAMs. The orientations of pentacene molecules deposited on SAMs bearing different terminal functional groups have been investigated by Hu *et al.*[10], and the experimental characterizations showed that the pentacene molecules nearly perpendicularly oriented on SAM functionalized gold (Au) surfaces but were parallel to the substrate surface on bare Au surface. The polar nature of SAMs can change the work function of the electrode by introducing surface dipoles, which allows the energy at the interface to be adjusted for realizing the tunable injection. For instance, Mei *et al.*[16] utilized the highly fluorinated SAMs to functionalize the surfaces of source and drain contacts in OFETs, and achieved the charge carrier mobilities as high as 5.7 $cm^2 V^{-1} s^{-1}$. Moreover, after applying alkylsilane SAMs like octadecylsilane (OTS) to treat the dielectric surfaces, the performance of OFETs can be ameliorated, which is attributed to the decrease of grain boundary number, the change of growth mode and the removal of hydroxy traps[11, 17-19]. In addition, some studies have also been reported that changing the terminal group of the SAMs to modify the interface between organic semiconductor and dielectric could profoundly exploit compatible organic-organic interactions to improve the device performance[20-21].

Apart from the improvement of electrical properties of devices by SAMs, the impact of SAMs on thermal properties at the interface is also worthy of paying more attention. The ability to dissipate Joule heat created by the device operation can affect the performance and life of electronic devices. However, owing to the weak vdW interaction across the metal electrode and organic layer, the inferior interfacial thermal transport at the interface hinders the heat dissipation. For example, by using the 3-ω method, the interfacial thermal conductances (ITCs) for Ag-copper phthalocyanine (CuPc) interface, Au-CuPc interface and Al-CuPc interface were experimentally measured to be 13±3 MW $m^{-2} K^{-1}$, 19±5 MW $m^{-2} K^{-1}$ and 50±15 MW $m^{-2} K^{-1}$, respectively[22-23]. In comparison with the ITCs of metal-inorganics interfaces reported

by Stevens *et al.*[24], the ITCs of metal-organics interfaces were less at least 10 times. Hence, understanding the mechanism of thermal energy transport at interface and developing the efficient strategy for reinforcing interfacial thermal transport are significant to further improve the performance of organic semiconductor electronic devices. A lot of studies have investigated thermal transport properties of some SAM modified interfaces[25-27]. Luo *et al*.[25] applied molecular dynamics (MD) method to simulate ITC of Au-SAM-Au junctions with alkanedithiols, showing the ITC values of around 200 ~ 300 MW m^{-2} K^{-1}. The interfacial thermal transports of water-solid interfaces functionalized with different SAMs were investigated by using time-domain thermoreflectance[26], and the experimental results exhibited that the thermal resistances at hydrophobic interfaces were 2~3 times larger than those of hydrophilic interfaces. The positive correlation between the chain length of SAMs and the interfacial thermal conductance of SAMs modified copper-carbon interfaces was observed by Hung *et al.*[27] Moreover, many researches demonstrate that the interfacial thermal conductance is strongly associated with the adhesion energy[28-29]. By using MD simulations, Shenogina *et al.* found the thermal conductance of SAM modified metal-water interface was proportional to the adhesion energy[29]. A similar experimental work of a series of alkanethiol monolayers conducted by Hari Krishna *et al.* also observed the proportional relationship between thermal conductance and work of adhesion[28]. Furthermore, the molecular polarity and hydrogen bonds can also affect the thermal transport across interfaces. Zhang *et al.* investigated the role of hydrogen bonds in thermal transports at hard-soft material interfaces and found that the more polarized SAMs leaded to a higher thermal conductance[30]. Another research conducted by Ma *et al.* also proved that the interfaces formed by boron nitride and polarized organic molecules possessed a higher ITC than the interfaces formed by nonpolarized organic molecules[31]. According to the aforementioned discussion, although the influence of SAMs on thermal transport has been reported, the interfacial thermal transport investigations of metal-SAM-organic semiconductor junctions are insufficient. Therefore, there is a desperate need to explore the interfacial thermal transport to guide the application of SAMs in organic electronic devices.

In this work, we perform the non-equilibrium molecular dynamics (NEMD) simulations to investigate thermal transport properties of metal-organic semiconductor interfaces. The thermal transport across four SAM functionalized interfaces are also investigated to study the impacts of terminal group of SAMs. We calculate the phonon density of states (PDOS) to uncover the underlying phonon transport mechanisms at interface, and analyze the intensities of interfacial interactions by calculating the interfacial adhesion energies, interfacial atom number densities, radial distribution functions and hydrogen bonds. It is found that the interfacial thermal transport is greatly enhanced by SAMs and the ITC enhancement is closely related to the polarity strength of terminal group of SAMs. The results of this study are expected to provide fundamental thermal knowledge on SAM modified metal interfaces and give the guidance to improve the performance of organic electronic devices.

2. Simulation Methods

In this work, we choose Au to act as the representative of metal, and the organic semiconductor is pentacene which has been widely applied in the organic electronics. Four kinds of thiol-terminated SAMs with different terminal groups are selected to functionalize the Au surface, including 1-hexanethiol [$HS(CH_2)_5CH_3$], 6-aminohexane-1-thiol [$HS(CH_2)_6NH_2$], 6-mercapto-1-hexanol [$HS(CH_2)_6OH$] and 6-mercaptohexanoic acid [$HS(CH_2)_5COOH$] (Fig. 1(a)). These SAM molecules have the same type of backbone (-CH_2-) and the same length of carbon chain. In this way, we can isolate the effects of backbone and length, and just focus on the effect of terminal groups. To concisely describe the SAM molecules in the following part, these SAMs are denoted as SAM(-CH_3), SAM(-NH_2), SAM(-OH) and SAM(-COOH), respectively. In MD simulations, Au atoms with a size of 60.56 × 29.97 × 89.90 Å^3 ($x \times y \times z$ Å^3) are modeled. The SAM molecules are placed on the (1 1 1) surface of Au, and form a ($\sqrt{3} \times \sqrt{3}$)R30^o full packing arrangement with a coverage of 21.60 Å^2 per SAM molecule[32]. The model of pentacene ($a \times b \times c$: 10 × 4 × 6 unit cells) is developed based on the crystal structure reported by Stefan[33]. The arrangement of pentacene model is that *a*

direction of pentacene along *x* direction and *b* direction in *x*-*y* plane. Due to the lattice constant mismatch between pentacene molecules and Au atoms, and in order to develop the atomic configuration of the system to form a periodic structure along *x* and *y* directions, the lattice constants of pentacene molecules are slightly modified, which induces a modification 1.65% for lattice constant *a* and -1.36% for lattice constant *b*.

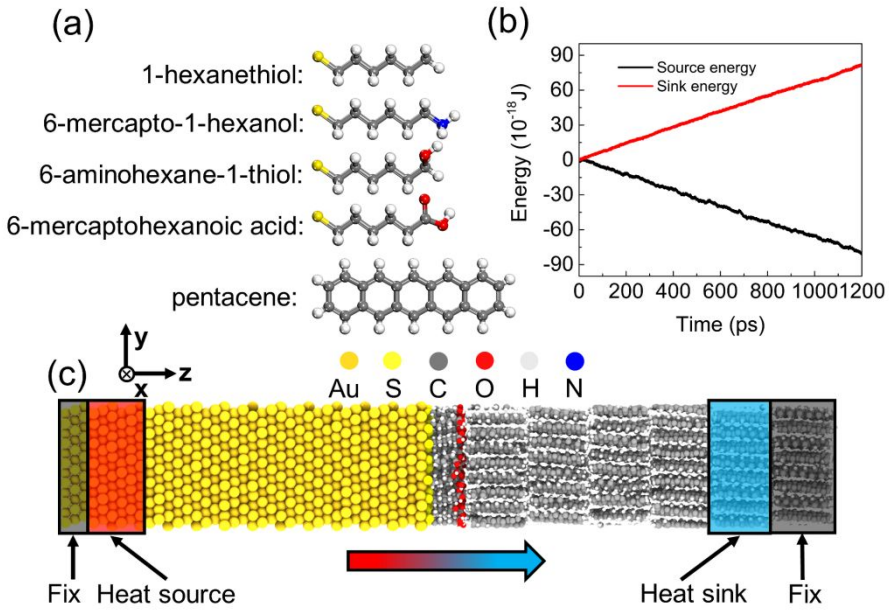

Figure 1. (a) Molecular structures of four SAM molecules and pentacene molecule. (b) The profiles of energy extracted from Langevin thermostats. (c) Schematic illustration of the simulation system composed of the Au surface functionalized by SAM(-COOH) and the pentacene molecules. Rectangular red and blue box represent heat source region and heat sink region in the NEMD process, respectively. The heat transports along *z* direction.

All MD simulations are performed by using the Large-scale Atomic/Molecular Massively Parallel Simulator (LAMMPS)[34]. The interaction parameters of SAM molecules are extracted from the polymer consistent force field (PCFF)[35], and the organic semiconductors are modeled by using the condensed-phase optimized molecular potentials (COMPASS)[36]. Both two force fields have been extensively used to simulate organic materials such as polymers[37], organic semiconductors[38-39], alkanes[40], and mercaptans[30]. Morse potential is used to describe the interaction among Au atoms and the interaction between Au atoms and sulfur (S) atoms[41]. The interactions between the Au atoms and organic material atoms (C, H, O, N) are modeled by the universal force field (UFF)[42], and the Lorentz-Berthelot mixing rules (ε_{ij}=sqrt($\varepsilon_i\varepsilon_j$) and

$\sigma_{ij}=(\sigma_i+\sigma_j)/2$) are used to calculate the energy parameter (ε) and distance parameter (σ) of UFF potential. The interaction of UFF is described as below:

$$E_{LJ} = 4\varepsilon\left[\left(\frac{\sigma}{r}\right)^{12} - \left(\frac{\sigma}{r}\right)^{6}\right] \quad (1)$$

where r is the distance between atoms. The timestep is set as 0.25 fs, owing to the faster vibrating hydrogen (H) atoms. The cutoff of 10 Å is chosen for Lenard-Jones (L-J) potential, and 8 Å for Morse potential. The periodic boundary conditions are applied in x and y directions, and the fixed boundary condition is applied in z direction.

To calculate the ITC between the Au and pentacene, NEMD simulations are performed. During MD simulations, the whole system is first equilibrated in canonical ensemble (NVT) for 0.5 ns at 300 K. During this NVT relaxation, the out-of-plane (z direction) stress at the interface can be released. After the system has been fully relaxed, the two outermost layer atoms are fixed. Other atoms except for the fixed atoms are equilibrated in NVT ensemble for another 0.5 ns, and then the system is switched under a micro-canonical ensemble (NVE) for 0.5 ns. In next 3.25 ns NEMD simulations, the atoms at both ends next to the fixed atoms are placed as heat sink and heat source regions. By using Langevin thermostats, the temperature of two thermostats are set as 250 K and 350 K for heat sink and heat source, respectively. After the temperature reaches the steady state, the temperature distribution and energy extracted from Langevin thermostats for last 1.25 ns are recorded to calculate ITC. The typical energy profile is shown in Fig. 1(b), and the heat flux (q) is calculated by averaging the energy input and output rates of the heat source and heat sink. The schematic illustration of the NEMD simulation setup is depicted in Fig. 1(c). Fig. 2 displays the temperature distributions of several models. The temperature drop (ΔT) at the interface is defined as the temperature difference between Au atoms and pentacene atoms that are nearest to the interface. We also utilize the linear extrapolation method to calculate the temperature drop, but we find that the linear extrapolation method may give rise to a smaller value for ΔT because of the layer-by-layer molecular orientation of pentacene. Therefore, the real temperature drop values at the interface are adopted to calculate ITCs in this work, and the ITC (G) is calculated as:

$$G = \frac{q}{\Delta T \cdot A} \tag{2}$$

where A is the cross-sectional area. We calculate five ITC values at different time blocks to obtain the average ITC values, and the error bars of ITC values are the standard deviations. In order to confirm the effect of system pressure on the ITC results, we also relax three representative structures (i.e. bare Au, SAM(-CH_3) functionalized structure, and SAM(-COOH) functionalized structure) at 1 atm in NPT ensemble before NVT and NVE ensembles. It is observed that the result discrepancies between with NPT relaxation and without NPT relaxation are negligible after considering the error bars of ITC values.

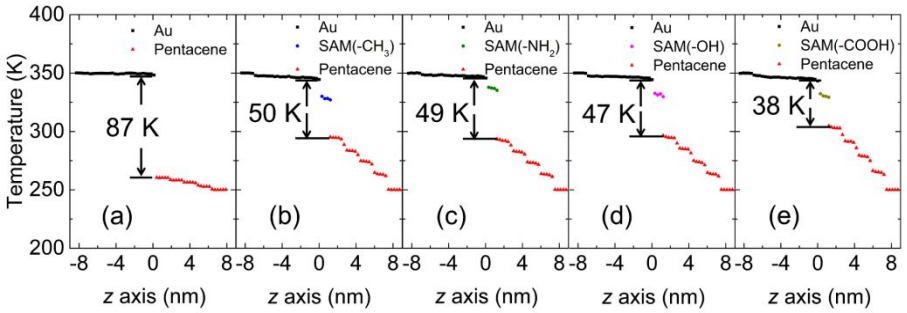

Figure 2. The typical temperature distributions of the system along *z* direction for (a) bare Au interface, (b) SAM(-CH_3) functionalized interface, (c) SAM(-NH_2) functionalized interface, (d) SAM(-OH) functionalized interface, and (e) SAM(-COOH) functionalized interface.

3. Results and Discussion

From five temperature distribution profiles for Au-pentacene interfaces functionalized by different SAMs in Fig. 2, it is observed that the temperature drops of interfaces between Au and pentacene are significantly reduced through functionalizing Au interfaces by SAMs. Especially, the interface modified by SAM(-COOH) possesses the lowest ΔT, which is reduced by 56.32% in comparison with the bare Au interface. Such small temperature drop indicates that the interface modified by SAM(-COOH) owns an excellent thermal conductance. We can also observe from the temperature profiles of pentacene that the energy transfer in the pentacene is layer by layer. The temperature difference is small in intraformational atoms but large in interlaminar

atoms of pentacene, which is the result of molecular crystal structure of pentacene.

The calculated ITC values are shown in Fig. 3(a). In Fig. 3(a), each color represents one type of functionalized surfaces by SAM molecules and the summarized values of some metal-other material interfaces of literature are also exhibited for comparison[26, 30, 40, 43-45]. The ITC value between bare Au and pentacene is 8.91±2.45 MW m^{-2} K^{-1}. It has been reported that the ITC between the bare Ag and DNTT measured by the experiment was 8.7 MW m^{-2} K^{-1} [43], and the slightly higher experimental value for Au-ethanol interface was 17.7 MW m^{-2} K^{-1} [44]. The ITC value of bare Au interface in our work is comparable to those of other metal-organics interfaces. By inserting SAM molecules, the interfacial thermal conductance is improved greatly in SAM modified interfaces. The ITC value for SAM(-CH_3) modified interface is 56.11±2.34 MW m^{-2} K^{-1}. The ITC value of SAM(-NH_2) modified interface is almost the same as the SAM(-CH_3) modified one. The SAM(-OH) displays a slightly better enhancement ability than SAM(-CH_3) and SAM(-NH_2), which brings about the ITC value of 65.78±3.62 MW m^{-2} K^{-1}. Furthermore, the ITC value of SAM(-COOH) modified interface is 101.15±6.02 MW m^{-2} K^{-1}, which is about 11 times larger than that of the bare Au interface. It is demonstrated that the SAM(-COOH) molecules have the best power to reinforce thermal transport for Au-pentacene interface. The variation trend among the different interfaces agrees with the MD study conducted by Zhang *et al.* [30] Our calculated ITC result of SAM(-CH_3) modified interface is in accordance with the reported experimental ITC values of Au-SAM-H_2O junction (50±5 MW m^{-2} K^{-1}) and Al-SAM-H_2O junction (60±5 MW m^{-2} K^{-1})[26]. The ITC values of SAM(-OH) and SAM(-COOH) modified interfaces are slightly lower than the values from references[26, 30]. Hence, we can draw two conclusions that all the four SAMs can enhance interfacial thermal transport and the SAM(-COOH) can improve the thermal conductance between Au and pentacene maximally.

To further analyze the process of energy transmission at interfaces, we separately calculate the ITC values of Au-SAM interfaces and SAM-pentacene interfaces, which are shown in Fig. 3(b). The ITCs of Au-SAM interfaces show the high values, which are consistent with the values of 200~400 MW m^{-2} K^{-1} reported by Luo *et al*. and Wang

et al.[46-47] The ITCs of SAM-pentacene interfaces are much lower than those of Au-SAM interfaces, which can be manifested by the large temperature differences between SAM molecules and pentacene molecules (see temperature distributions in Fig. 2). It is seen that when the more polarized SAMs are used, the ITC values of Au-SAM interfaces and SAM-pentacene interfaces are raised. For Au-SAM interfaces, the Au atoms are rigidly connected to S atoms by covalent bonds, which allows energy to transmit from Au atoms to SAM molecules efficiently. Thus, the main resistance of interfacial thermal transport locates at the interfaces between SAM and pentacene. The ITC of SAM modified interfaces can be decomposed into the following equation:

$$\frac{1}{ITC_{total}} = \frac{1}{ITC_{Au-SAM}} + \frac{1}{ITC_{SAM-pentacene}} \quad (3)$$

Since $ITC_{Au\text{-}SAM}$ is much larger than $ITC_{SAM\text{-}pentacene}$, the equation indicates that the effective method to improve ITC_{total} is to enlarge $ITC_{SAM\text{-}pentacene}$, which can be realized by changing the terminal group of SAM to construct the better thermal coupling interfaces.

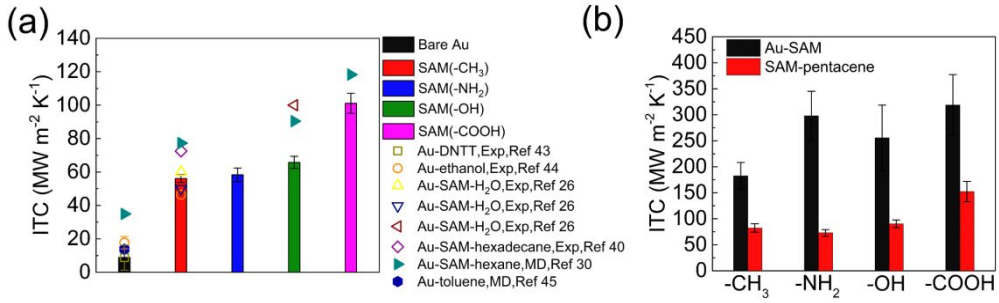

Figure 3. (a)The calculated interfacial thermal conductances of bare Au interface and four SAM functionalized interfaces. The open scatter symbols represent the summarized experimental ITC values of references.[26, 40, 43-44] The solid scatter symbols represent the summarized MD values of references.[30, 45](b) The interfacial thermal conductances of Au-SAM and SAM-pentacene interfaces for different SAM functionalized interfaces.

In general, many special treatments, such as oxygen plasma treatment[48-50], annealing temperature[51-53] and deposition substrate temperature[54] can tune the surface energy. By utilizing those methods, the vdW interaction between the substrate and organic semiconductors is further ameliorated. Herein, we also investigate the effect of

interfacial coupling strength by varying the L-J energy interaction parameters (ε) between Au atom and other atoms (C, H, O, N) from 1 to 3 times. We choose three representative interfaces to investigate this effect and the calculated results are shown in Fig. 4. It can be seen that the interfacial thermal conductance of bare Au increases linearly when the L-J energy interaction parameter is augmented. The ITC value of bare Au interface with the triple L-J energy parameter is 57.19±3.26 MW m^{-2} K^{-1}, which is very close to value of the interface modified by SAM(-CH_3). It is worthy to note that the ITCs of two SAM functionalized Au interfaces almost unchanged even if the L-J energy parameter is tripled. The interaction mechanism between Au and SAM molecules can account for that phenomenon. The bare Au-pentacene interface is connected by weak vdW interactions, which means that varying the L-J energy parameters easily improves the interaction between bare Au atoms and pentacene molecules. However, the effect of covalent bonds between Au atoms and S atoms for SAM functionalized interfaces is much larger than that of increasing L-J energy parameters. Therefore, for SAM modified interfaces, changing L-J energy parameters makes little impact on the interfacial thermal transport.

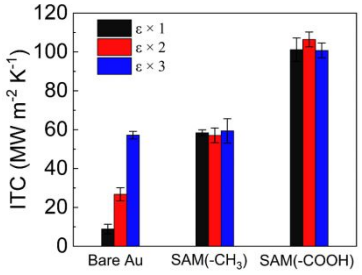

Figure 4. The interfacial thermal conductances of bare Au interface, SAM(-CH_3) and SAM(-COOH) functionalized interfaces under different L-J energy interaction parameters.

According to the acoustic mismatch and diffusive mismatch models, the better matched vibrational modes between two materials give rise to the higher thermal conductance[55-56]. PDOS provides valuable physical insights for the thermal transport properties of the different materials. By taking the Fourier transformation of the velocity autocorrelation function, the PDOS is calculated by:

$$P(\omega)=\frac{1}{\sqrt{2\pi}}\int_{-\infty}^{\infty}e^{-i\omega t}\frac{\langle v(t)\cdot v(0)\rangle}{\langle v(0)\cdot v(0)\rangle}dt \quad (4)$$

where the $P(\omega)$ is the PDOS at the frequency of ω, and $v(t)$ and $v(0)$ are atom velocity at t time and zero time, respectively. By analyzing the frequency distribution of PDOS, the differences of phonon transport mechanism for different materials are revealed. The overlapping degree of PDOS at interface indicates the thermal transport coupling capacity between the two different materials. The calculated PDOS of Au, four different SAMs, and pentacene are shown in Fig. 5. It can be observed that the vibrational frequency range of Au atoms distributes in the low frequency region (< 10 THz) but the pentacene possesses less vibrational frequency in the low frequency region. Hence, a large vibrational mismatch between Au and pentacene atoms leads to the inferior interfacial thermal transport. Merabia *et al*. adopted a generalization of the acoustic mismatch model to calculate the phonon transmission coefficients between Au-water interface which also had low thermal conductance, and found that the transmission coefficients almost distributed below 10 THz[57]. Our calculated PDOS of Au and pentacene is in accordance with the results of Merabia *et al*. Because the chemical compositions of SAMs are similar, the PDOS of four SAMs resembles each other. It is observed that the vibrational frequencies of four different SAMs match better with Au atoms in the low frequency region compared with pentacene. The largely populated low frequency (< 10 THz) phonon modes between Au atoms and SAMs are caused by the Morse interaction between the Au and S atoms[25], which is induced by strong covalent bonds. In addition, because both SAMs and pentacene are organic materials, SAM molecules and pentacene have a similar PDOS distribution in whole frequency range. The favorable overlapping of PDOS can result in a better vibrational coupling between the two materials, which makes thermal transport more efficient. The larger PDOS coupling between SAMs and pentacene makes energy transport from SAMs to pentacene easier than that from Au to pentacene. By using phonon wave packet simulations, Wei *et al.* demonstrated that phonon energy transmission coefficients at Au-SAM(-CH_3)-hexane junction were larger than those of Au-hexane junction, and the thermal conductance was proportional to phonon energy transmission coefficient[58].

Therefore, the SAM molecules imbedded in the middle of Au and pentacene can play the role of "phonon bridge" to fill the gap between Au and pentacene in vibrational spectra, which broadens energy transport channels between Au and pentacene. Consequently, the thermal transport efficiency for Au-SAM-pentacene junction is heightened.

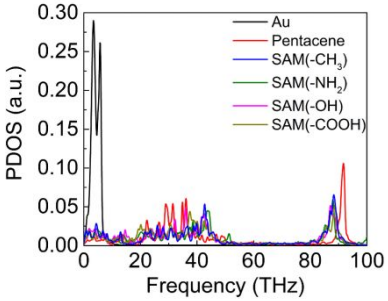

Figure 5. The calculated PDOS of Au, different SAMs and pentacene.

Although the PDOS of four SAMs is similar, the ITC values of SAM modified interfaces with different terminal groups are diverse. According to the previous work[59-60], it can be believed that the different ITC enhancements are ascribed to the different intensities of interfacial interactions. To uncover the intensities of interfacial interactions, the interfacial adhesion energy between pentacene and functionalized Au (Au + SAM) is calculated by summing all interactions across the interfaces in MD simulations as shown in Fig. 6. There are obvious differences in interfacial adhesion energies between four SAMs. The interfaces modified by SAM(-CH_3) and SAM(-NH_2) have almost the same interfacial adhesion energies, which can interpret the similar ITC values. Owing to the polarization characteristics, SAM(-OH) and SAM(-COOH) possess the larger interfacial adhesion energies. The interfacial adhesion energies of interfaces modified by SAM(-OH) and SAM(-COOH) are -130.22±15.99 Kcal mol^{-1} and -209.98±15.41 Kcal mol^{-1}, respectively. Another interesting observation is that the interfacial adhesion energy of bare Au interface is larger than those of SAM(-CH_3) and SAM(-NH_2). It is necessary to mention that the adhesion energies of bare Au and functionalized Au (Au + SAM) interfaces are based on different potentials. More importantly, as discussed above, the SAM molecules can bring about better vibrational coupling to enhance thermal transport. Thus, although the interfaces modified by

SAM(-CH_3) and SAM(NH_2) have lower interfacial adhesion energies, the SAM(-CH_3) and SAM(-NH_2) modified interfaces possess higher ITC values than that of bare Au interface. Therefore, we can conclude that different thermal conductance enhancements of SAM(-CH_3), SAM(-NH_2), SAM(-OH) and SAM(-COOH) are attributed to the increase in interfacial adhesion energy.

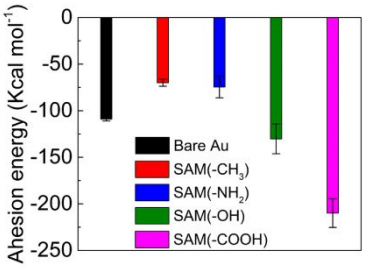

Figure 6. The interfacial adhesion energies of bare Au interface and four SAM functionalized interfaces.

Furthermore, to expound the interaction strength between SAM molecules and pentacene, the calculated atom number densities near the interfaces are displayed in Fig. 7. Along *z* direction that is normal to the interface, the model is divided into thousands of slabs with a thickness of 0.1 Å. The position of interface between SAMs and pentacene is defined as the position of local minimum atom number density. To expediently compare the atom number density, the interface positions of four different SAMs are adjusted to 0 Å. We find that there is a space of about 2 Å without atoms for the bare Au interface. In comparison with the bare Au interface, the SAM functionalized Au interfaces have higher atom number densities near the interface and shorter lengths of space without atoms. The peaks of atom number density for SAM functionalized interfaces are also pulled closer to interface. Particularly, the SAM(-COOH) modified interface has the highest atom number density near the interface, which accounts for the highest value of ITC. Since the stronger interface interactions can pull the pentacene molecules closer to the SAM molecules, the high atom number density and the number of pair interactions near the interface will increase, which is beneficial to the energy transmission across the interface.

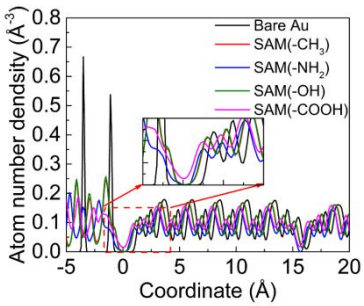

Figure 7. The atom number densities near the different interfaces. The interface positions of four different SAM functionalized interfaces are placed to 0 Å.

Additionally, we also calculate the radial distribution functions (RDFs) of the representative groups of SAMs (-CH_3 group, -CH_2NH_2 group, -CH_2OH group and -COOH group) with respect to H atoms in pentacene molecules. It is seen from Fig. 8 that the first peak in RDF of SAM(-COOH) appears earlier than other SAMs, which means the interaction distance between -COOH group and H atoms of pentacene is shorter. The RDF curves of SAM(-COOH) and SAM(-OH) exhibit obvious peaks and valleys, which can illustrate the well arrangement of pentacene molecules due to the strong interfacial interactions. The distances of first and second peaks of those two SAMs are calculated, which are 2.02 Å for SAM(-COOH) and 2.18 Å for SAM(-OH). Especially, the first peak in RDF of SAM(-COOH) is higher than other SAMs. Those also demonstrate that the SAM(-COOH) can interact with pentacene molecules powerful. Unlike the RDFs of SAM(-COOH) and SAM(-OH), the RDF curves of SAM(-CH_3) and SAM(-NH_2) are smoother, and the peaks and valleys are not obvious. Those phenomena indicate that the laminated structure of pentacene is feeble at weak interaction interfaces.

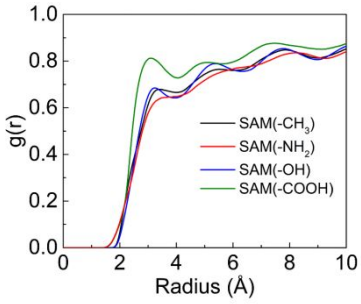

Figure 8. Radial distribution functions of four representative groups on SAMs (-CH_3 group, -CH_2NH_2 group, -CH_2OH group and -COOH group) with respect to H atoms in pentacene

molecules.

As discussed above, the interactions between the pentacene and the Au interfaces modified by SAM(-COOH) and SAM(-OH) are more forceful, which reminds us whether there are hydrogen bonds between the SAM molecules and pentacene. Many studies have proved that the existence of hydrogen bonds could vastly improve interfacial thermal conductance[26, 60-61]. The probable type of hydrogen bond in interfaces of SAMs and pentacene is CH···O hydrogen bond. Gu *et al.* demonstrated that although the CH···O hydrogen bond was weak, it was a true hydrogen bond and the distance of C···O was around 3.5 Å[62]. Here, the visual molecular dynamics (VMD)[63] is used to calculate the number of hydrogen bonds with the following criteria: (1) The distance between the donor and the acceptor of the hydrogen bond is less than 3.5 Å; (2) The angle of hydrogen bond is less than 40°. The number of hydrogen bonds is exhibited in Fig. 9. It can be found that the hydrogen bond number of SAM(-COOH) modified interface is larger than the number of SAM(-OH) modified interface, which is well corresponding to the higher interfacial adhesion energy of SAM(-COOH). The existence of hydrogen bond will also make atoms at the interface closer, which further confirms the high atom number density at the SAM(-COOH) interface. In short, the supreme enhancement of the interfacial thermal transport of SAM(-COOH) can attributed to the better vibrational coupling at interface and the more intense interfacial interactions at SAM-pentacene interface caused by the polarized terminal group.

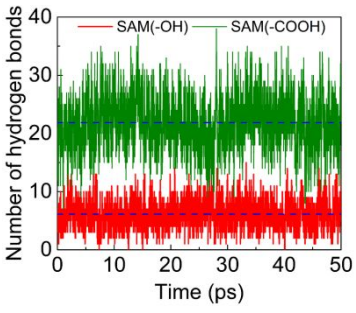

Figure 9. The numbers of hydrogen bonds of SAM(-OH) and SAM(-COOH) functionalized interfaces. The dash lines are the average numbers of hydrogen bonds.

4. Conclusions

In this work, the non-equilibrium molecular dynamics simulations are performed to study the thermal energy transport at Au-SAM-pentacene interfaces. The effects of four SAMs with different terminal groups on interfacial thermal transport are investigated. The ITC of bare Au interface is 8.91±2.45 MW m^{-2} K^{-1}. The ITC values of SAM functionalized Au interfaces are enhanced greatly by SAMs. The ITC values of SAM(-CH_3), SAM(-NH_2), SAM(-OH) and SAM(-COOH) modified Au interfaces are 56.11±2.34 MW m^{-2} K^{-1}, 58.35±4.01 MW m^{-2} K^{-1}, 65.78±3.62 MW m^{-2} K^{-1} and 101.15±6.02 MW m^{-2} K^{-1}, respectively. The SAMs with polarization groups exhibit the better reinforcement in ITC. We ascribe the ITC enhancement by SAMs to the better phonon vibrational coupling and stronger interfacial interactions. By calculating PDOS, we find that the SAMs can act as "phonon bridge" to broaden energy transport channels between Au and pentacene and result in the higher ITC. Additionally, we further evaluate the adhesion energies at interfaces and find that the SAM(-COOH) modified Au interface has the uppermost adhesion energy. The atom number densities and RDFs at interfaces are also estimated and analyzed, which testify that the stronger interactions at interface induce the higher adhesion energy and the more regular arrangement of pentacene molecules at interface. Afterwards, we calculate the numbers of hydrogen bonds at SAM(-OH)-pentacene and SAM(-COOH)-pentacene interfaces. It is found that the more polarized interface exhibits more powerful cohesion and then brings about the better interface transmission capacity. Our findings demonstrate that modifying the metal surface by SAMs can significantly enhance ITC of metal-organic semiconductor interface, and this work is expected to provide valuable information for the thermal management in organic electronic devices.

Conflicts of interest

There are no conflicts of interest to declare.

Acknowledgments

The authors gratefully acknowledge the support from the National Natural Science Foundation of China (No. 51806123), the Natural Science Foundation of Shandong Province, China (No. ZR2018BEE025), the Natural Science Foundation of Guangdong Province, China (No. 2020A1515010686), the China Postdoctoral Science Foundation (No. 2018M642654) and the Fundamental Research Funds of Shandong University, China (No. 2018TB007).

References

1. Chen, J.; Yang, K.; Zhou, X.; Guo, X., Ladder-Type Heteroarene-Based Organic Semiconductors. *Chemistry–An Asian Journal* **2018**, *13*, 2587-2600.
2. Xugang, G.; Antonio, F.; Marks, T. J., Imide- and Amide-Functionalized Polymer Semiconductors. *Chemical Reviews* **2014**, *114*, 8943-9021.
3. Wang, C.; Dong, H.; Jiang, L.; Hu, W., Organic Semiconductor Crystals. *Chemical Society Reviews* **2018**, *47*, 422-500.
4. Sirringhaus, H., 25th Anniversary Article: Organic Field-Effect Transistors: The Path Beyond Amorphous Silicon. *Advanced Materials* **2014**, *26*, 1319-1335.
5. Quinn, J. T. E.; Zhu, J.; Li, X.; Wang, J.; Li, Y., Recent Progress in the Development of N-Type Organic Semiconductors for Organic Field Effect Transistors. *Journal of Materials Chemistry C* **2017**, *5*, 8654-8681.
6. Huang, W., et al., Uv–Ozone Interfacial Modification in Organic Transistors for High-Sensitivity No2 Detection. *Advanced Materials* **2017**, *29*, 1701706.
7. Fritz, S. E.; Kelley, T. W.; Frisbie, C. D., Effect of Dielectric Roughness on Performance of Pentacene Tfts and Restoration of Performance with a Polymeric Smoothing Layer. *The Journal of Physical Chemistry B* **2005**, *109*, 10574-10577.
8. Huang, F.; Cheng, Y.-J.; Zhang, Y.; Liu, M. S.; Jen, A. K. Y., Crosslinkable Hole-Transporting Materials for Solution Processed Polymer Light-Emitting Diodes. *Journal of Materials Chemistry* **2008**, *18*, 4495-4509.

9. Chu, C.-W.; Li, S.-H.; Chen, C.-W.; Shrotriya, V.; Yang, Y., High-Performance Organic Thin-Film Transistors with Metal Oxide/Metal Bilayer Electrode. *Applied Physics Letters* **2005**, *87*, 193508.
10. Hu, W. S.; Tao, Y. T.; Hsu, Y. J.; Wei, D. H.; Wu, Y. S., Molecular Orientation of Evaporated Pentacene Films on Gold: Alignment Effect of Self-Assembled Monolayer. *Langmuir* **2005**, *21*, 2260-2266.
11. Virkar, A. A.; Mannsfeld, S.; Bao, Z.; Stingelin, N., Organic Semiconductor Growth and Morphology Considerations for Organic Thin-Film Transistors. *Advanced Materials* **2010**, *22*, 3857-3875.
12. Kim, H.; Meihui, Z.; Battaglini, N.; Lang, P.; Horowitz, G., Large Enhancement of Hole Injection in Pentacene by Modification of Gold with Conjugated Self-Assembled Monolayers. *Organic Electronics* **2013**, *14*, 2108-2113.
13. Hamadani, B. H.; Corley, D. A.; Ciszek, J. W.; Tour, J. M.; Natelson, D., Controlling Charge Injection in Organic Field-Effect Transistors Using Self-Assembled Monolayers. *Nano Letters* **2006**, *6*, 1303-1306.
14. Kang, B.; Jang, M.; Chung, Y.; Kim, H.; Kwak, S. K.; Oh, J. H.; Cho, K., Enhancing 2d Growth of Organic Semiconductor Thin Films with Macroporous Structures Via a Small-Molecule Heterointerface. *Nature Communications* **2014**, *5*.
15. Ma, H.; Acton, O.; Hutchins, D. O.; Cernetic, N.; Jen, A. K. Y., Multifunctional Phosphonic Acid Self-Assembled Monolayers on Metal Oxides as Dielectrics, Interface Modification Layers and Semiconductors for Low-Voltage High-Performance Organic Field-Effect Transistors. *Physical Chemistry Chemical Physics* **2012**, *14*, 14110-14126.
16. Mei, Y.; Fogel, D.; Chen, J.; Ward, J. W.; Payne, M. M.; Anthony, J. E.; Jurchescu, O. D., Interface Engineering to Enhance Charge Injection and Transport in Solution-Deposited Organic Transistors. *Organic Electronics* **2017**, *50*, 100-105.
17. Lee, H. S.; Kim, D. H.; Cho, J. H.; Hwang, M.; Jang, Y.; Cho, K., Effect of the Phase States of Self-Assembled Monolayers on Pentacene Growth and Thin-Film

Transistor Characteristics. *Journal of the American Chemical Society* **2008**, *130*, 10556-10564.

18. Shin, T. J.; Yang, H.; Ling, M.-m.; Locklin, J.; Yang, L.; Lee, B.; Roberts, M. E.; Mallik, A. B.; Bao, Z., Tunable Thin-Film Crystalline Structures and Field-Effect Mobility of Oligofluorene–Thiophene Derivatives. *Chemistry of Materials* **2007**, *19*, 5882-5889.
19. Yang, H.; Shin, T. J.; Yang, L.; Cho, K.; Ryu, C. Y.; Bao, Z., Effect of Mesoscale Crystalline Structure on the Field-Effect Mobility of Regioregular Poly(3-Hexyl Thiophene) in Thin-Film Transistors. *Advanced Functional Materials* **2005**, *15*, 671-676.
20. Salleo, A.; Chabinyc, M. L.; Yang, M. S.; Street, R. A., Polymer Thin-Film Transistors with Chemically Modified Dielectric Interfaces. *Applied Physics Letters* **2002**, *81*, 4383-4385.
21. Tsukagoshi, K.; Shigeto, K.; Yagi, I.; Aoyagi, Y., Interface Modification of a Pentacene Field-Effect Transistor with a Submicron Channel. *Applied Physics Letters* **2006**, *89*, 113507.
22. Jin, Y.; Yadav, A.; Sun, K.; Sun, H.; Pipe, K. P.; Shtein, M., Thermal Boundary Resistance of Copper Phthalocyanine-Metal Interface. *Applied Physics Letters* **2011**, *98*, 093305.
23. Jin, Y.; Shao, C.; Kieffer, J.; Pipe, K. P.; Shtein, M., Origins of Thermal Boundary Conductance of Interfaces Involving Organic Semiconductors. *Journal of Applied Physics* **2012**, *112*, 093503.
24. Stevens, R. J.; Smith, A. N.; Norris, P. M. J. J. H. T., Measurement of Thermal Boundary Conductance of a Series of Metal-Dielectric Interfaces by the Transient Thermoreflectance Technique. *Journal of Heat Transfer* **2005**, *127*, 315-322.
25. Luo, T.; Lloyd, J. R., Equilibrium Molecular Dynamics Study of Lattice Thermal Conductivity/Conductance of Au-Sam-Au Junctions. *Journal of Heat Transfer* **2009**, *132*, 032401.
26. Ge, Z.; Cahill, D. G.; Braun, P. V., Thermal Conductance of Hydrophilic and Hydrophobic Interfaces. *Physical Review Letters* **2006**, *96*, 186101.

27. Hung, S.-W.; Hu, S.; Shiomi, J., Spectral Control of Thermal Boundary Conductance between Copper and Carbon Crystals by Self-Assembled Monolayers. *ACS Applied Electronic Materials* **2019**, *1*, 2594-2601.

28. Harikrishna, H.; Ducker, W. A.; Huxtable, S. T., The Influence of Interface Bonding on Thermal Transport through Solid–Liquid Interfaces. *Applied Physics Letters* **2013**, *102*, 251606.

29. Shenogina, N.; Godawat, R.; Keblinski, P.; Garde, S., How Wetting and Adhesion Affect Thermal Conductance of a Range of Hydrophobic to Hydrophilic Aqueous Interfaces. *Physical Review Letters* **2009**, *102*, 156101.

30. Zhang, T.; Gans-Forrest, A. R.; Lee, E.; Zhang, X.; Qu, C.; Pang, Y.; Sun, F.; Luo, T., Role of Hydrogen Bonds in Thermal Transport across Hard/Soft Material Interfaces. *ACS Applied Materials & Interfaces* **2016**, *8*, 33326-33334.

31. Ma, R.; Wan, X.; Zhang, T.; Yang, N.; Luo, T., Role of Molecular Polarity in Thermal Transport of Boron Nitride–Organic Molecule Composites. *ACS Omega* **2018**, *3*, 12530-12534.

32. Widrig, C. A.; Alves, C. A.; Porter, M. D., Scanning Tunneling Microscopy of Ethanethiolate and N-Octadecanethiolate Monolayers Spontaneously Absorbed at Gold Surfaces. *Journal of the American Chemical Society* **1991**, *113*, 2805-2810.

33. Schiefer, S.; Huth, M.; Dobrinevski, A.; Nickel, B., Determination of the Crystal Structure of Substrate-Induced Pentacene Polymorphs in Fiber Structured Thin Films. *Journal of the American Chemical Society* **2007**, *129*, 10316-10317.

34. Plimpton, S., Fast Parallel Algorithms for Short-Range Molecular Dynamics. *Journal of Computational Physics* **1995**, *117*, 1-19.

35. Sun, H.; Mumby, S. J.; Maple, J. R.; Hagler, A. T., An Ab Initio Cff93 All-Atom Force Field for Polycarbonates. *Journal of the American Chemical Society* **1994**, *116*, 2978-2987.

36. Sun, H., Compass: An Ab Initio Force-Field Optimized for Condensed-Phase Applicationsoverview with Details on Alkane and Benzene Compounds. *The Journal of Physical Chemistry B* **1998**, *102*, 7338-7364.

37. Zhang, T.; Wu, X.; Luo, T., Polymer Nanofibers with Outstanding Thermal Conductivity and Thermal Stability: Fundamental Linkage between Molecular Characteristics and Macroscopic Thermal Properties. *The Journal of Physical Chemistry C* **2014**, *118*, 21148-21159.

38. Martinelli, N. G., et al., Influence of Intermolecular Vibrations on the Electronic Coupling in Organic Semiconductors: The Case of Anthracene and Perfluoropentacene. *ChemPhysChem* **2009**, *10*, 2265-2273.

39. Chen, J.; Anthony, J.; Martin, D. C., Thermally Induced Solid-State Phase Transition of Bis(Triisopropylsilylethynyl) Pentacene Crystals. *The Journal of Physical Chemistry B* **2006**, *110*, 16397-16403.

40. Sun, F.; Zhang, T.; Jobbins, M. M.; Guo, Z.; Zhang, X.; Zheng, Z.; Tang, D.; Ptasinska, S.; Luo, T., Molecular Bridge Enables Anomalous Enhancement in Thermal Transport across Hard-Soft Material Interfaces. *Advanced Materials* **2014**, *26*, 6093-6099.

41. Wei, X.; Zhang, T.; Luo, T., Molecular Fin Effect from Heterogeneous Self-Assembled Monolayer Enhances Thermal Conductance across Hard–Soft Interfaces. *ACS Applied Materials & Interfaces* **2017**, *9*, 33740-33748.

42. Rappe, A. K.; Casewit, C. J.; Colwell, K. S.; Goddard, W. A.; Skiff, W. M., Uff, a Full Periodic Table Force Field for Molecular Mechanics and Molecular Dynamics Simulations. *Journal of the American Chemical Society* **1992**, *114*, 10024-10035.

43. Wang, X.; Parrish, K. D.; Malen, J. A.; Chan, P. K. L., Modifying the Thermal Conductivity of Small Molecule Organic Semiconductor Thin Films with Metal Nanoparticles. *Scientific Reports* **2015**, *5*, 16095.

44. Tian, Z.; Marconnet, A.; Chen, G., Enhancing Solid-Liquid Interface Thermal Transport Using Self-Assembled Monolayers. *Applied Physics Letters* **2015**, *106*, 211602.

45. Kikugawa, G.; Ohara, T.; Kawaguchi, T.; Torigoe, E.; Hagiwara, Y.; Matsumoto, Y., A Molecular Dynamics Study on Heat Transfer Characteristics at the Interfaces of Alkanethiolate Self-Assembled Monolayer and Organic Solvent.

The Journal of Chemical Physics **2009**, *130*, 074706.

46. Wang, Z.; Carter, J. A.; Lagutchev, A.; Koh, Y. K.; Seong, N.-H.; Cahill, D. G.; Dlott, D. D., Ultrafast Flash Thermal Conductance of Molecular Chains. *Science* **2007**, *317*, 787-790.
47. Luo, T.; Lloyd, J. R., Non-Equilibrium Molecular Dynamics Study of Thermal Energy Transport in Au–Sam–Au Junctions. *International Journal of Heat and Mass Transfer* **2010**, *53*, 1-11.
48. Song, B. J.; Hong, K.; Kim, W.-K.; Kim, K.; Kim, S.; Lee, J.-L., Effect of Oxygen Plasma Treatment on Crystal Growth Mode at Pentacene/Ni Interface in Organic Thin-Film Transistors. *The Journal of Physical Chemistry B* **2010**, *114*, 14854-14859.
49. Kim, W.-K.; Lee, J.-L., Effect of Oxygen Plasma Treatment on Reduction of Contact Resistivity at Pentacene/Au Interface. *Applied Physics Letters* **2006**, *88*, 262102.
50. Lee, M. W.; Song, C. K., Oxygen Plasma Effects on Performance of Pentacene Thin Film Transistor. *Japanese Journal of Applied Physics* **2003**, *42*, 4218-4221.
51. Guo, D.; Ikeda, S.; Saiki, K.; Miyazoe, H.; Terashima, K., Effect of Annealing on the Mobility and Morphology of Thermally Activated Pentacene Thin Film Transistors. *Journal of Applied Physics* **2006**, *99*, 094502.
52. Ye, R.; Baba, M.; Suzuki, K.; Ohishi, Y.; Mori, K., Effect of Thermal Annealing on Morphology of Pentacene Thin Films. *Japanese Journal of Applied Physics* **2003**, *42*, 4473-4475.
53. Wang, X.; Peng, B.; Chan, P., Thermal Annealing Effect on the Thermal and Electrical Properties of Organic Semiconductor Thin Films. *MRS Advances* **2016**, *1*, 1637-1643.
54. Jung, M.-C.; Leyden, M. R.; Nikiforov, G. O.; Lee, M. V.; Lee, H.-K.; Shin, T. J.; Takimiya, K.; Qi, Y., Flat-Lying Semiconductor–Insulator Interfacial Layer in Dntt Thin Films. *ACS Applied Materials & Interfaces* **2015**, *7*, 1833-1840.
55. Cahill, D. G., et al., Nanoscale Thermal Transport. Ii. 2003–2012. *Applied Physics Reviews* **2014**, *1*, -.

56. Swartz, E. T.; Pohl, R. O., Thermal Boundary Resistance. *Reviews of Modern Physics* **1989**, *61*, 605-668.

57. Merabia, S.; Lombard, J.; Alkurdi, A., Importance of Viscoelastic and Interface Bonding Effects in the Thermal Boundary Conductance of Solid–Water Interfaces. *International Journal of Heat and Mass Transfer* **2016**, *100*, 287-294.

58. Wei, X.; Luo, T., A Phonon Wave Packet Study of Thermal Energy Transport across Functionalized Hard-Soft Interfaces. *Journal of Applied Physics* **2019**, *126*, 015301.

59. Wei, X.; Zhang, T.; Luo, T., Thermal Energy Transport across Hard–Soft Interfaces. *ACS Energy Letters* **2017**, *2*, 2283-2292.

60. Zhang, L.; Bai, Z.; Liu, L., Exceptional Thermal Conductance across Hydrogen-Bonded Graphene/Polymer Interfaces. *Advanced Materials Interfaces* **2016**, *3*, 1600211.

61. Patel, H. A.; Garde, S.; Keblinski, P., Thermal Resistance of Nanoscopic Liquid−Liquid Interfaces: Dependence on Chemistry and Molecular Architecture. *Nano Letters* **2005**, *5*, 2225-2231.

62. Gu, Y.; Kar, T.; Scheiner, S., Fundamental Properties of the CH···O Interaction: Is It a True Hydrogen Bond? *Journal of the American Chemical Society* **1999**, *121*, 9411-9422.

63. Humphrey, W.; Dalke, A.; Schulten, K., Vmd: Visual Molecular Dynamics. *Journal of Molecular Graphics* **1996**, *14*, 33-38.

Table of Contents Image

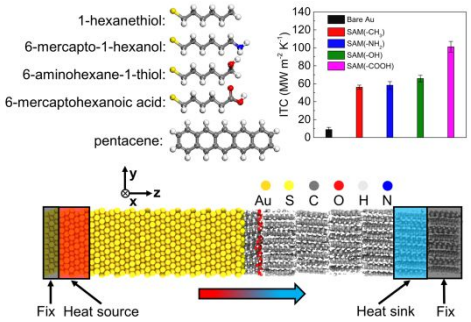

We pioneer the probing into the enhancement mechanism of interfacial thermal transport between metal and organic semiconductor by self-assembled monolayers.